Enabling Holistic Tracking and Tracing in Battery Cell Production: Marking Technologies and Identification

Alessandro Sommer[*a], *Hakon Gruhn*[*b], *Alexander Schoo*[c], *Malte Mund*[b], *Steffen Bazlen*[d], *Hai-Yen Tran*[d], *Maja W. Kandula*[b], *Klaus Dilger*[b], *Wolfgang Braunwarth*[d], *and Rüdiger Daub*[a,e]

[a] Technical University of Munich, TUM School of Engineering and Design
Institute for Machine Tools and Industrial Management (*iwb*)
Boltzmannstrasse 15, 85748 Garching, Germany
E-Mail: Alessandro.sommer@iwb.tum.de

[b] Technical University of Braunschweig, Institute of Joining and Welding (ifs)
Langer Kamp 8, 38106 Braunschweig, Germany
E-Mail: h.gruhn@tu-braunschweig.de

[c] Technical University of Braunschweig, Institute of Particle Technology (iPat)
Langer Kamp 19b, 38106 Braunschweig, Germany

[d] Center for Solar Energy and Hydrogen Research Baden-Wuerttemberg (ZSW),
Lise-Meitner-Strasse 24, 89081 Ulm, Germany

[e] Fraunhofer Institute for Casting, Composite and Processing Technology (IGCV)
Am Technologiezentrum 10, 86159 Augsburg, Germany

Abstract

The production of battery cells involves a complex process chain with interconnected steps leading to unknown cause-and-effect relationships and production inaccuracies, contributing to costly scrap due to expensive materials. An integrated traceability system down to the level of single electrode sheets allows the linkage of intermediate products and their measured properties throughout the entire process chain. This approach creates a new database that improves the understanding of interactions within the process chain. For a traceability system, a unique identification of the intermediate products is required. Therefore, this work introduces a four-step methodology for seamlessly integration of relevant components into the battery cell production process to ensure traceability. Laser and ink-based markings are described in detail, and the readability is evaluated depending on the marking parameters. For all methods, the advantages and challenges are outlined. Laser and ink marking systems are suitable options for the unique identification of intermediate products. The markings can be decoded with devices along the process chain, which is an efficient solution. Image-based methods enable marking-free identification of intermediate products but require a significantly more complex hardware technology in each process step for a comprehensive traceability system.

DOI: 10.14459/2024mp1764299

1. Introduction

Climate change drives the need to convert the energy production and transportation sectors to renewable energy sources.[1] In the transportation sector, electrochemical energy storages play a decisive role in replacing fossil-fueled technologies. Lithium-ion batteries (LIBs) are a suitable energy storage solution for automotive applications due to their high energy density. As a result, the demand for LIBs as the dominant energy storage solution is constantly increasing.[2] Simultaneously, there is a noticeable increase in quality and sustainability standards for batteries, driven by the European Green Deal and intensifying market demands. Consequently, it is crucial to enhance the quality of cells and minimize manufacturing scrap in the production process. The high complexity of battery cell manufacturing complicates this task.[3] The manufacturing of LIB cells involves a continuous material flow and various production steps.[3] Notably, due to the substantial material expenses, one of the most significant challenges in production is the sensitivity of battery cell costs to potential production errors or inaccuracies.[4] Traditional quality management practices, such as conventional batch tracing, often prove insufficient for targeted defect elimination.[5] To enhance transparency in battery cell production, especially in the continuous processes, it is important to increase data granularity.[6] To unveil unknown cause-and-effect relationships responsible for manufacturing inaccuracies and high scrap rates, digitization approaches like data-driven methods are increasingly emphasized in the literature, which require high data quality and consistent, product-specific data mapping to fully exploit their potential.[7–9] All these methods require a high standard of data quality and consistent data allocation specific to the product to maximize their potential. Variations in manufacturing processes within LIB production often lead to inconsistent production datasets.[5,9,10] The documentation of traceability approaches in battery cell production remains limited in the literature. Nevertheless, the industry has recognized this challenge.[11] The clear traceability of a product and all its associated information is becoming increasingly important within the progress of digitization. According to ISO 9000:2015, traceability is defined as the capability to follow the history, application, or location of an object. In this context both, tracking and tracing (T&T), are of central importance. Tracking involves real-time monitoring of the whereabouts and status of items as they progress through various stages of a supply chain or distribution network. It relies on technologies such as Radio-Frequency Identification or barcodes to provide continuous updates on the location, movement, and condition of products. Traceability refers to the ability to reconstruct the historical path and particulars of a product's journey through the supply chain, capturing and preserving a record of all events, processes, and interactions the product undergoes from its origin to its destination. Tracing is proving to be essential for quality control, regulatory compliance, and dealing with issues such as recalls or quality defects. T&T hold the potential to notably enhance data quality within battery cell production. By closely monitoring material and component movement through the production process (tracking) and meticulously reconstructing the historical journey and details of each product (tracing), battery cell manufacturers can achieve better transparency and accuracy in their production processes. This comprehensive approach facilitates the identification and elimination of defects, accountability establishment, and process optimization, ultimately leading to enhanced overall quality and efficiency in battery cell manufacturing. RIEXINGER et al. previously emphasized the necessity of implementing a T&T system to accurately link production data with intermediate products. In the context of electrode manufacturing, the electrode coil is identified through applied product ID, while the electrode stack or cell is marked and recognized as the traceability object during cell assembly and finalization.[11] WESSEL et al. incorporated a T&T system within the continuous improvement Plan-Do-Check-Act (PDCA) process.[12] This system is intended to associate accumulating production data with increasing value creation to enable data-driven approaches with consistent data sets. However, in continuous processes like roll-to-roll electrode coating and calendering, traceability systems have only been implemented in a limited manner so far.[13] For the precise linkage of production data with intermediate products, the intermediate product must be uniquely identified to establish a traceable resource unit (TRU).[12] Subsequently, WESSEL et al. proposed that ink markings or feature-based attributes of electrodes can be employed to automatically identify individual electrode sheets. This newly created fine-grained database can then be harnessed for data-driven strategies to reinforce quality management and gain deeper insights into process-product relationships.[14] SOMMER et al. suggested that by integrating a marking strategy at the beginning of electrode production, it is possible to assign product and process data to each electrode sheet produced during coating, drying, calendering, and electrode sheet separation processes.[15] It is noteworthy that these approaches have remained primarily theoretical and lack concrete evidence for a physical implementation of a T&T system. In this context, SOMMER et al. experimentally demonstrated that the integration of a marking to facilitate T&T is indeed achievable[16], considering the mutual impact of the process chain and the marking.[17] Furthermore, it was demonstrated that a marking can be integrated in real-time during electrode production, allowing for the segmentation and allocation of production data to individually marked electrode sections.[18] Furthermore, the assigned data could be used to explain anomalies in the cell cycling.[19] The literature collected shows that it is essential for a comprehensive T&T system to allocate production data to individual intermediate products.

The subject of traceability has been investigated from diverse perspectives with varying levels of detail in recent years. This study is intended to provide a comprehensive overview on the topic and serve as a guideline for implementing a T&T system in the battery industry. Knowledge and literature on T&T in battery production are reviewed and supplementary tests are carried out to ensure comprehensive recommendations on the design and use of T&T systems. The aim of this part is to give instructions for the integration of a T&T system focusing on the hardware components and their implementations. This includes marking-based identifications using laser and ink systems as well as non-marking camera systems. To emphasize the practical benefits of a traceability system, potential use cases are presented.

2. Methodology for the implementing of a marker-based T&T system

A crucial aspect of a complete T&T system is the clear identification of intermediate products, which is essential for the continuous recording of the production processes. Markings enable unambiguous identification of intermediate products, facilitating traceability for the so-called TRU. Direct part marking is a structured approach used for implementing such a marking-based system, ensuring accurate T&T in battery cell production.

Developing a reliable and marker-based T&T system for electrode and cell manufacturing requires a systematic approach, as shown in **Figure 1**. The process begins with defining the system's purpose and constraints, specifying the type of information to be encoded, such as ID, production dates, batch numbers, and determining the desired level of traceability, down to single electrodes. Environmental and operational constraints such as processes, machinery, material properties, space limitations, and lighting conditions must be identified.

Next, based on the information to be stored and the identified limitations, the appropriate coding scheme and marking technology must be selected. Appling codes is recommended for its versatility, with the size of the code depending on implications on other process steps and the data to be

DOI: 10.14459/2024mp1764299

stored. Factors such as marking system durability, costs, and flexibility are considered.
The reading device must be chosen based on code quality, compatibility with the selected code type, operational environment, decoding speed, and costs. Practical tests showed that adjustments to the marking systems or readers are necessary to ensure optimal performance within defined constraints. Iterative refinement ensures the development of an efficient T&T system capable of effective tracking and identification throughout the production process.

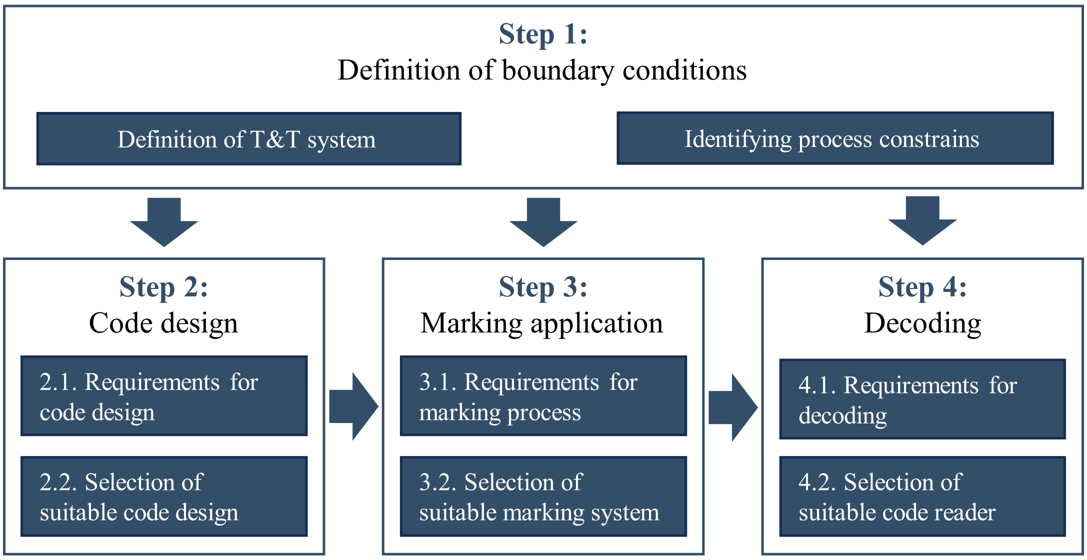

Figure 1: Illustration of the structured approach for the implementation of a T&T system. Based on the definition of boundary conditions (step 1), code design (step 2), marking application (step 3), and decoding (step 4) are derived in a continuous process with respect to the defined boundary conditions and the previous implementation step.

The following sections give detailed information on the implementation process and practical advises based on the experiences of the authors. The method resulted from studies carried out on the integrability of markings in the manufacturing process of LIBs as part of the *TrackBatt* research project. In addition to the steps presented, exemplary studies are shown which provide a deeper understanding.

2.1. Step 1: Definition of boundary conditions

The integration of a marking for a T&T system should take place as early as possible in the process chain of battery production to establish a consistent link between recorded data and the intermediate products. Within the continuous process steps of electrode production, crucial product parameters are defined that significantly influence cell performance.[3] Therefore, traceability of production data should be implemented already in the electrode manufacturing stage. For this purpose, the coating process has already been identified as a suitable integration point.[15] In the discrete process steps after stacking, only marking on the cell housings is required for a comprehensive traceability system. For the cell housing marking, Data Matrix Codes (DMCs) are already commonly used in the industry as a standard practice.[20,21]

.

The boundary conditions depend on the material properties, the process properties, the specified code data, the electrode configurations, and application specific regulations and specifications, as shown in **Figure 2**. These five areas constitute the boundary conditions and will be considered in the following sections.

DOI: 10.14459/2024mp1764299

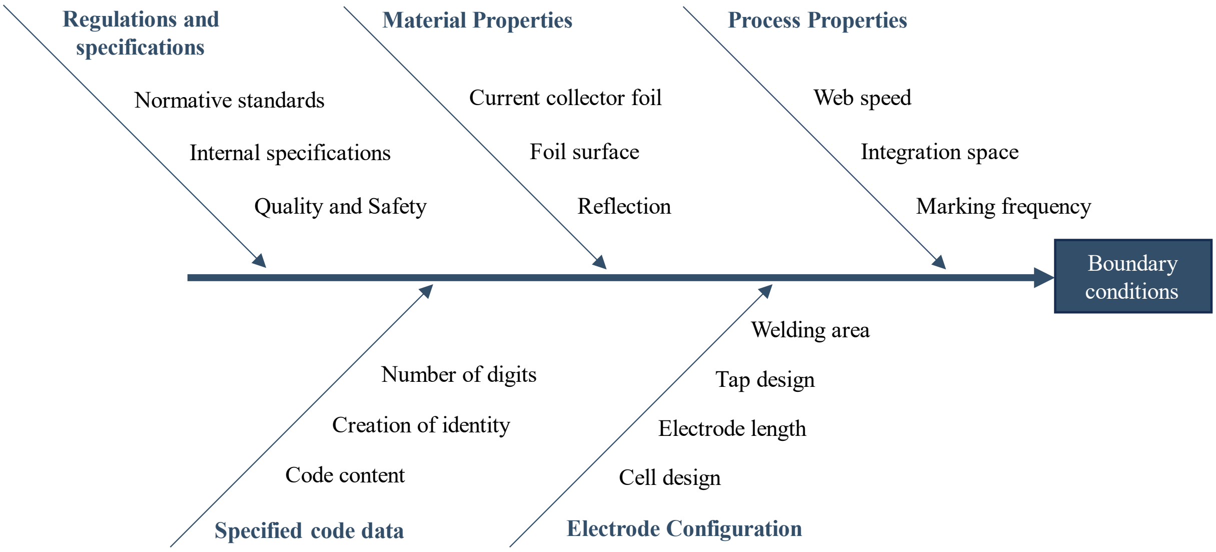

Figure 2: Impact factors on a T&T system in electrode manufacturing, which define the boundary conditions.

It is essential to determine the information intended to be stored in the code. The target is to generate a unique ID through the code content. It must be specified at the beginning whether data that goes beyond a unique ID, like a batch ID, is to be stored in the markings. The specified data is central for the implementation of a T&T system, as it forms the basis for the selection of a suitable code and suitable marking technology and code readers.

The manufacturing processes for the electrodes and the cell assembly must be clearly defined. Marking and decoding highly depends on the manufacturing speed and both, marking and decoding hardware must be selected accordingly. Especially the web speed plays a crucial role in the utilization of an inline-capable traceability system. It defines the temporal sequence of production speeds and directly influences the rate at which markings can be applied to intermediate products and subsequently decoded. The available installation space in the machinery for electrode production must be evaluated, as this determines the maximum dimensions of the marking and code reader. Understanding cell assembly is crucial as specific production steps like stacking and contacting can impact code selection and dictate requirements for marking and code reader.

Knowledge about the material properties of the current collector is crucial, as they have a significant influence on both the marking and decoding processes. In addition to the material type, surface properties such as reflectivity, and surface roughness also have a major influence on manufacturability and readability. Therefore, comprehensive information on the current collectors is mandatory.

In addition, it is necessary to define the marking distance for the T&T system in electrode production. It must be decided whether the system is tailored for one type of battery (prismatic cell, round cell, or pouch cell), a specific electrode size, or whether it accommodates a range of formats. The required marking and decoding frequency highly depend on the battery cell type, the electrode size and the speed of the process, as exemplary shown in **Figure 3** where the dependence of marking frequency on the web speed for different code distances is illustrated.

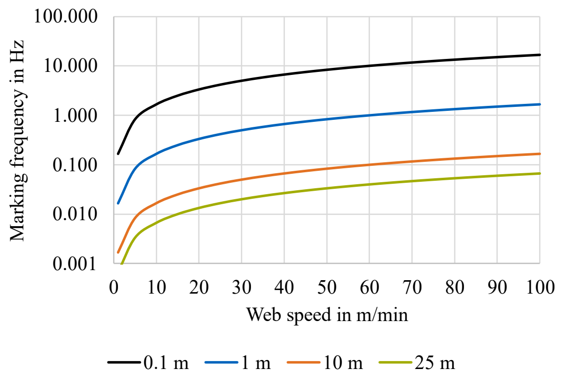

Figure 3: Marking frequency depending on the web speed and the code distance.

The marking frequency increases with increasing web speed. Furthermore, a smaller marking distance requires a significantly higher marking frequency than a larger one. For the code readers, this also means that less time is available for decoding the marking at higher web speeds and smaller code distances.

Another aspect considers the user-specific regulations and specifications. For instance, a widespread standard is ISO/IEC 16022, which describes the Data Matrix symbology and its associated quality parameters. The standard specifies the Data Matrix symbology characteristics, data character encoding, symbol formats, dimensions and print quality requirements, error correction rules, decoding algorithm, and user-selectable application parameters.[22] In accordance with the described parameters, an applied DMC receives a grading for each category ranging from A to F. A represents the best possible rating, while F signifies the worst possible rating with the code remaining readable. In summary, a DMC receives a global grading, which is determined by the lowest rating among all criteria. The size of the code should be chosen so that it can be produced as part of the electrode production process and readability is reliably possible. This sets a further boundary that must be considered during the whole implementation process. Another important point involves workplace safety. It is essential to ensure that integrated marking systems are in line with the safety measures prevailing on-site. For instance, laser safety is worth mentioning here.

2.2. Step 2: Code design

DMCs and quick response (QR) codes are widely used for their efficient data storage and easy scanning with mobile devices. These codes are two-dimensional (2D) barcodes. They offer compact storage for large amounts of information, which is useful when marking space is limited. The codes consist of dark squares (modules) and light squares arranged in a square or rectangular pattern. The cell size refers to the size of the individual modules or squares that make up the code and is typically measured in units such as millimeters or pixels, depending on whether the code is printed on a physical object or digitally displayed. Their fast readability allows quick data capture and processing with code readers or smartphones. They are durable enough to be printed or engraved on various surfaces and withstand production and logistics processes. Both formats include error correction for accurate decoding even with damage. Implementing DMC or QR codes can be cost-effective compared to other tracking methods.

2.2.1. Requirements for code design

The type of code and its size define the design of the code. Requirements for both parameters are derived from the boundary conditions.

Data storage capacity:

- The primary requirement for the code size on a battery cell or electrode is its capacity to store the defined data set. This includes critical information like a unique ID, Batch ID, manufacturing dates, and potentially additional parameters.
- The code size is related to the data quantity and the type of code specified during the initial boundary condition definition.

Minimum code size constraints:

- Data accommodation: The code must possess sufficient storage capacity to store the entire defined data set without loss or truncation.
- Readability: The code format and size need to be optimized for readability on the chosen cell format and size. A balance is required between maximizing data storage and ensuring ease of decoding during cell and electrode inspection.

Maximum code size constraints:

- Available marking area: The cell format dictates the available surface area suitable for code placement. Cylindrical and prismatic cells potentially offer uncoated regions for marking, while pouch cells have a limited marking area confined to their current collector flag size.
- Readability: Thermal distortions by laser marking increase with bigger DMC and can negatively affect the decoding time.
- Cell functionality: This means that the applied markings should not excessively affect the current collector foils or joining zones mechanically, nor should the applied markings dissolve in the electrolyte and negatively impact cell performance.

2.2.2. Selection of suitable code design

The choice of the type of code mainly depends on the defined amount of data to be stored. One-dimensional (1D) or 2D barcodes are suitable. The difference between 1D barcodes and 2D barcodes is the amount of data that can be stored. As 2D barcodes are able to store data in both the horizontal and the vertical dimension, they are capable of storing over 100 times more data than typical 1D barcodes.[23] Comparisons of potential 2D barcodes showed that the DMC provided the most information within a given space.[17]. At this point, the DMC is recommended due to its high storage capacity. For example, a DMC with 14 x 14 modules can store 16 integers, sufficient for a unique ID in most cases. However, other code formats can also meet the requirements, considering the other boundary conditions.

2.3. Step 3: Marking application

The application of markings or DMCs can be carried out through ink or laser-based systems. Those solutions were investigated within the scope of this work and the research project *TrackBatt*. These technologies are already widely used in the industry for component labeling in T&T applications. Since the systems have different requirements as well as advantages and disadvantages, they are considered in a differentiated manner in this work.

Laser marking is a widely used industrial application of laser systems. When the laser beam interacts with the surface of the substrate, various physical processes occur, allowing for the application of a highly durable and legible marking.[24] There are three main methods for applying a marking on a product surface: raster marking, vector marking, and marking using a mask. In all these methods, the laser beam follows a 2D trajectory on the object's surface. [25] The marking process is synchronized with the movement of the object, whether it's stationary or in motion, which is determined by the operation of the laser system or the application of laser marking.[25] To ensure proper marking, the distance between the laser system and the object must remain constant or within an approved range to maintain focus. Laser engraving involves the removal of material, necessitating extraction.[25] Safety measures, including design measures and classifications, must be adhered to when working with laser systems.[26]

As an alternative technology, inkjet printing technology has undergone development for numerous applications in the past three decades, including product date codes, mailing materials, desktop printing, large-area graphics, and, most recently, the direct deposition of materials to create electronic, biological, polymeric, and metallic devices.[27] Although all inkjet technologies can be fundamentally defined as the digitally controlled ejection of fluid drops from a

DOI: 10.14459/2024mp1764299

print head onto a substrate, the methods employed vary. Industrial inkjet is commonly and broadly categorized as either continuous (CIJ) or drop-on-demand (DOD), with variations within each classification.[28]

However, both systems, laser and ink, share the commonality that a unique information is stored in the code itself through the applied marking, which is later used to distinguish intermediate products. The following sections define the requirements for both processes and recommend a procedure for selecting a suitable marking method as step 3 of the implementation process.

2.3.1. Requirements for marking application

The requirements for the marking process can be categorized into two main aspects: those concerning the marking device and process itself, and the quality standards for the codes applied. The applied codes must meet the quality standards outlined in the boundary conditions to ensure readability. It is imperative that the marking process can consistently produce codes of the specified quality. The requirements for both the marking process and the marking device can be inferred directly from these boundary conditions. The codes should be applied early to a physically traceable intermediate product to ensure consistent linkage of production data throughout the process chain.[15] For this purpose, the application of the code to the current collector foil is recommended to apply during the coating process. To avoid an additional marking process step, the marking should be applied inline in the coating machine.[18] This results in two further requirements:

Properties of a marking device:

- The maximum size of the marking device is set from the available space in the machinery.
- The marking speed must keep pace with the coating speed. Generally, coating speeds vary from 25 to 50 m min^{-1}.[29,30] Achieving the desired marking frequency is crucial for fulfilling the requirements for the T&T system. This frequency is determined by a combination of factors, including the chosen DMC size and the inherent properties of the marking technology.

As an example, experiments with a laser system (MD-X2500A, Keyence, Japan) regarding the marking speed were carried out. Due to mirror inertia in a laser marking process, the optics scanner's speed is limited, which prevents unlimited reduction of marking time. Hence, when the web speed is fixed, the distance between markings cannot be set arbitrarily; instead, a minimum distance is determined by the required marking time. This is analogous to the findings of SOMMER et al [15]. This system revealed a marking time of 0.88 s for DMCs with 12 x 26 modules on copper with a cell size of 0.36 mm, enabling web speeds of 8.5 m min^{-1}. However, the current process time of 0.88 s is insufficient for industrial applications due to the limited marking field size of the laser system. Scaling up to a laser with a marking field of 300 x 300 mm would only marginally increase the possible web speed to over 20 m min^{-1}, still not meeting the desired throughput. Additionally, this would result in a code distance of 300 mm, rendering individual electrode sheet tracking impractical in many instances. To address these limitations, the most effective approach is to reduce the process time by minimizing the number of modules and their size. By transitioning from 12 x 26 modules with a cell size of 0.36 mm to 16 x 16 modules with a cell size of 0.3 mm, the process time can be reduced to 0.31 s using the same process parameters e.g., scanning speed of 3500 mm s^{-1}. A DMC with 16 x 16 modules can accommodate 24 integers, providing sufficient data storage for individual electrode sheet tracking. Future advancements in laser systems, higher scanning speeds, and optimized filling patterns can further reduce the process time to less than 0.1 s for copper foils, demonstrating the potential of laser marking to achieve the necessary marking speed for individual electrode sheet tracking in industrial settings. The laser marking process of aluminum foil is, due to the higher absorptivity and lower melting point, faster.

DOI: 10.14459/2024mp1764299

As the marking is located on the current collectors, it may be present in the joining zone for contacting depending on the electrode format. This is especially relevant for stacked electrodes. The marking process should not negatively impede the contacting process. Therefore, the impact of the marking on electrical conductivity and mechanical strength needs to be investigated.

Influence on the joining zone:

- The marking must not have a negative or non-acceptable influence on the mechanical strength of the joining zone.
- The marking must not have a negative or non-acceptable influence on the electrical conductivity of the joining zone.

Two examples are given below where an ink-based and a laser-based marking were placed in the welding area and welded by ultrasonic welding. In both examinations, the used codes were DMCs with 12 x 26 modules and the same cell size of 0.36 mm. The experiments were conducted with an ultrasonic spot welder (Branson L20 Emerson, Ferguson, USA) and a 7 x 11 mm horn. For the welding process 10 foils were stacked and welded with a 200 µm arrester tab. The welding parameters for copper were set to 150 J welding energy, 1500 N welding pressure, 47 µm amplitude and for aluminum to 110 J, 1500 N, 47 µm respectively. The results of the investigation are shown in **Figure 4**.

The first example was based on a laser-based marking process. The material removal and surface roughening induced during laser marking led to notch effects. Hence, tensile tests of current collectors pre-marked with the laser system revealed reduced strengths, as shown in **Figure 4a**. When welding on the markings, the DMC can protrude above the joint, fully activating the notch effect. The notch effects can also be observed in the welded specimens, shown in **Figure 4b.** Therefore, the laser-marked DMC should be fully covered by the welding area. With the 12 x 26 DMC, no substantial negative impacts on mechanical properties were observed, as shown in **Figure 4c**.

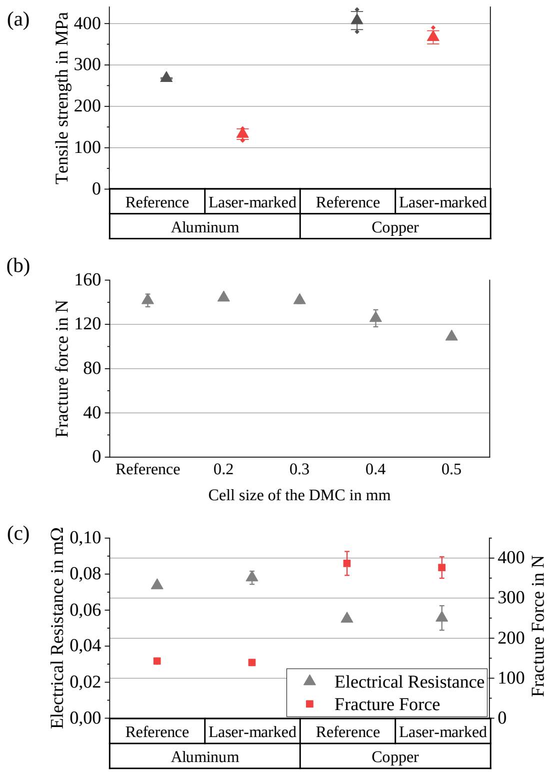

Figure 4: Examinations of the impact of laser markings on the properties of the foils and welds: tensile strength of blank current collectors after laser marking with 16 x 16 modules and 0.4 mm cell size in (a), impact of the weakening due to the laser marking on the ultrasonic weld strength in dependence of the cell size in (b), and comparison of the weld properties with laser-marked DMC with 12 x 26 modules with unmarked current collector welds in (c).

Another example was welded with the same welding parameters and setup, but on ink-marked current collectors. The experiments revealed a marginally negative impact of the ink, shown in **Figure 5**. This resulted in a slight reduction in fracture force while simultaneously increasing scatter. Electrical resistance also changed from approximately 0.050 mΩ to 0.064 mΩ. This is attributed to the altered friction behavior in the areas of ink marking, leading to divergent weld properties following the ultrasonic welding process. Consequently, it is imperative to adjust the welding parameters to accommodate the modified tribology. In the case of aluminum foils, a substrate fracture occurred in the current collector tabs for both unmarked reference and ink-marked foils, indicating that the joint were not critically affected. Nevertheless, individual tests must be conducted with the intended ink to prove that there is no negative influence of the marking on the electrochemical performance, as the chemical composition of the ink is generally unknown or not provided by the suppliers.

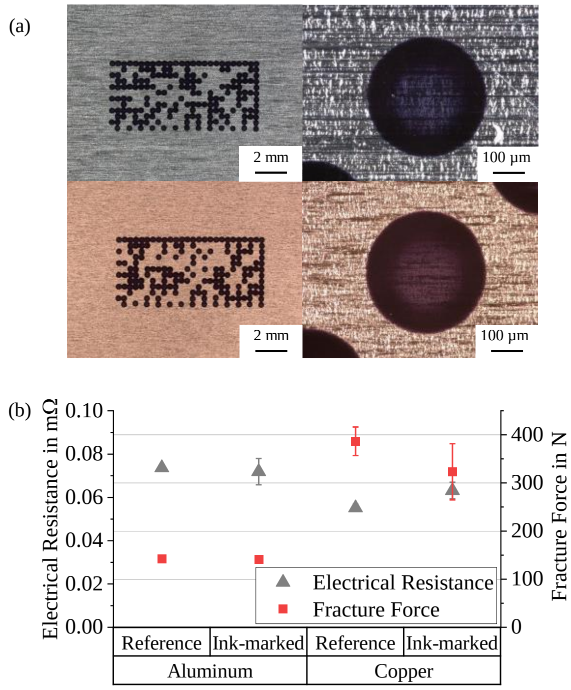

Figure 5: Illustration and enlargement of the ink marking on aluminum and copper foil in (a) and analysis of the impact of ink-marked DMC with 12 x 26 modules on the properties of ultrasonically welded foils in (b).

Besides these general requirements, there are specific requirements for ink-based and laser-based marking processes. While ink-based processes are quite robust and do not depend on material properties, the requirements for laser marking are quite high. Thus, the successful marking of the current collectors' hinges on the selection of an appropriate laser system. It is required, that the laser-based marking can apply codes with a sufficient quality on the defined materials.

2.3.2. Selection of suitable marking technology

The selection of the suitable marking devices and process require a general decision whether to use a laser-based or an ink-based marking system. Both, ink and laser marking can effectively meet the marking requirements for T&T in battery cell production. This is demonstrated by the fact that other process steps are not significantly disrupted, and the cell properties are retained in the absence of significant disruptions to other process steps and the preservation of cell properties. Nevertheless, individual tests should be carried out regarding the quality of the codes applied, the processability of marked electrodes and in the case of ink systems, the impact on the battery cell performance. Additionally, for laser marking, the integration effort is significantly higher, reflected in the elevated capital expenses. Conversely, laser marking is characterized by its wear-free operation and reduced operating expenses, which makes it attractive for large scale production. Furthermore, marking time could be an obstacle, which requires careful evaluation and selection of a suitable marking system. The basic advantages and disadvantages of both systems are given in **Table 1**.

Table 1: Advantages and disadvantages of laser-based and ink-based marking systems.

	Laser-based	Ink-based
Advantage	• Flexible in code design and position • Low maintenance • No operating expenses	• High marking frequency • Low investment costs • Easy installation
Disadvantage	• High investment costs • Additional safety requirements	• Ink contact with electrolyte • Operation costs due to ink consumption

Selection of suitable devices for laser-based marking

When choosing to implement laser-based markings, several additional considerations must be made. In general, three distinct wavelength ranges are conceivable: the infrared (IR) range with approximately 1064 nm wavelength, the green range, and the ultraviolet (UV) range. The green and UV wavelengths are often achieved by

DOI: 10.14459/2024mp1764299

frequency doubling via second harmonic generation or tripling of the infrared wavelength.[31] The wavelength significantly influences the absorption rate of radiation by different materials. A high absorption rate facilitates the marking process. However, frequency doubling also reduces the maximum achievable laser power, potentially counteracting the benefits of high absorption. Marking with IR lasers requires a high peak pulse power but is still the most cost-effective option, enabling the marking of both aluminum and copper.[32–34] **Figure 6** illustrates the absorption behavior of various metals for the three different laser wavelengths of 355 nm, 532 nm, and 1064 nm.

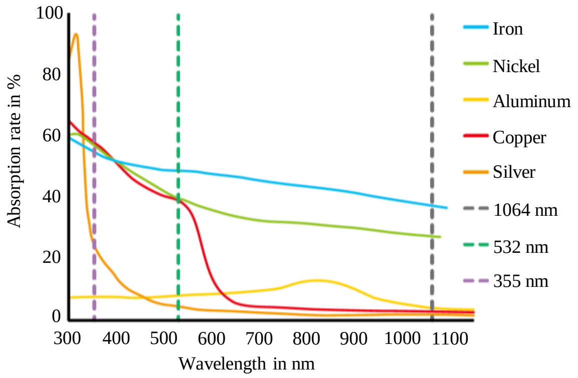

Figure 6: Absorption rates of different metals in dependence on the wavelength of the laser system, modified from [35].

The extended wavelength of infrared lasers reduces the Rayleigh length, rendering the laser system more sensitive to focus deviations. Compensating for these deviations by increasing the working distance results in a larger pulse diameter and decreased focus ability, potentially compromising the marking process. The power density decreases while the average power remains constant, further hindering the marking effectiveness.[36] Therefore, achieving a small spot diameter requires a stable focus position. If necessary, this must be ensured by additional web deflections.

The laser-material interactions between aluminum and copper exhibit substantial disparities, manifested notably in marking time. Laser marking with an IR wavelength on aluminum is significantly shorter. This difference stems not solely from the higher absorption rate but also from aluminum's lower melting point of the aluminum and enhanced reactivity with oxygen, necessitating lower peak pulse powers for marking compared to copper. The contrast of the DMC on aluminum is created by surface roughening and the formation of an oxide layer, identifiable by a dull white color.[37] Conversely on copper, tempering colors primarily provide contrast, accompanied by significantly lower material removal at comparable marking performance.[38]

Selection of suitable devices for ink-based marking

Ink-based marking requires additional considerations due to its potential impact on material properties and long-term durability. If the ink marking is present on the current collector foils, which subsequently comes in contact with the electrolyte in the assembled state in the battery cell, the marking may dissolve in the solvents of the electrolyte. Consequently, the electrolyte may be contaminated with ink. Therefore, the impact of the dissolved ink on the electrochemical performance of the battery cell needs to be assessed. Initial investigations have shown that there is no significant difference between cells with and without contamination in the electrolyte.[17] However, no long-term studies have been conducted so far. Furthermore, it is generally recommended to avoid the detachment of ink codes into the electrolyte. The dyes may contain graphite-like components that can become electrochemically active.

2.4. Step 4: Decoding

For all process steps involving the tracking of intermediate products such as electrodes, a code reader is necessary for tracking. The code readers available in the industry differ from one another not only in their features but also significantly in their costs. Hence, it is prudent to understand the requirements for the code reader to procure suitable devices without incurring unnecessary expenses. There are several commercially

DOI: 10.14459/2024mp1764299

available code readers that are suitable for a marker-based T&T system in electrode and cell production. Key characteristics of code readers include the maximal resolution, the internal exposure, the recording frequency, and the software and integrated hardware such as working memory and processor performance.[39] Furthermore, it is noteworthy that code readers must be implemented at all process steps of the battery production chain as a part of the T&T system.

2.4.1. Requirements for decoding

Production and web speed:

- The DMCs must be decoded during the processes to track the intermediate products. Consequently, the code readers used must also keep pace with the process speeds of the production steps. In the calendering process, process speeds of up to 100 m min^{-1} occur[3], which represents the highest demand on the web speed and thus the reading speed in continuous processes.
- The decoding time of the codes must be correspondingly shorter than the required processing time of the electrode section in each step, e.g. calendaring or electrode stacking.

Exposure:

- Particular attention must be paid to the exposure, as the current collector foils have a high reflectivity. The code readers should be installed in places with little ambient light.
- With fixed DMC design and exposure, the decoding time that can be achieved is set by the performance of the code readers.

Code reader specifications:

- The code readers' resolution, in conjunction with the size of the code cells, determines the achievable operating distance and working field. Simultaneously, resolution is the code reader attribute that most significantly impacts costs, as higher resolution correlates with increased code reader performance.
- Other significant specifications include recording frequency, implemented digital interfaces, as well as the scope and performance of the software. Many manufacturers use their artificial intelligence to improve code reading capabilities. Therefore, it is advisable to test potential reading devices individually.

As already mentioned, a crucial factor for code readability on aluminum and copper foil is primarily the exposure. The high reflectivity of the foils results in certain areas of the field of view where the code becomes unreadable under direct illumination. Therefore, there should be as little extraneous light as possible in the reading process section. Furthermore, this issue can be improved by using polarized or diffuse light. Tests conducted with a code reader (SR-X300, Keyence, Japan) illustrate this. **Figure 7** shows the same laser-marked DMC on aluminum and copper foil with different exposure options. In this case, it was possible to fully compensate for the unintended reflection due a direct exposure of the foils using polarization to enhance readability. With this, decoding times below 40 ms for the shown ink- and laser-marked DMC with ratings according to ISO/IEC TR29159 between A and B were achieved. The integrated software of the code reader was not trained on the codes, only the exposure and focus were adjusted.

DOI: 10.14459/2024mp1764299

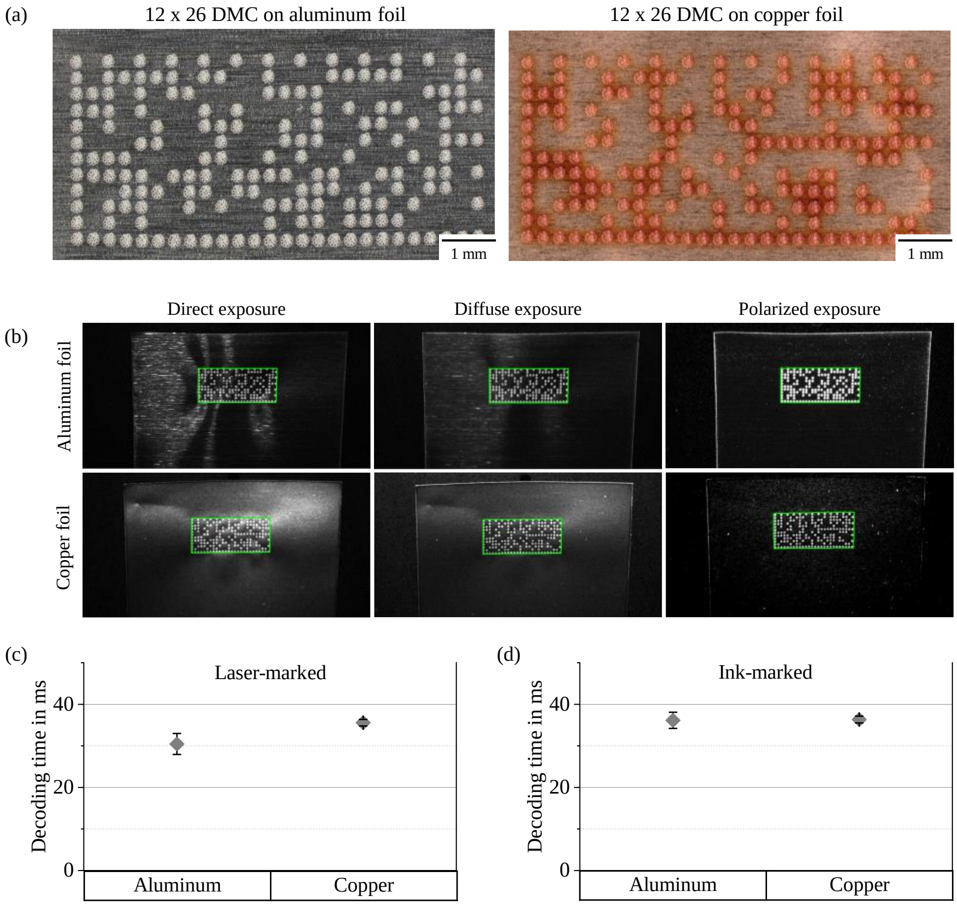

Figure 7: Laser-marked DMC with 12 x 26 modules on aluminum and copper foil in (a), images taken by the code reader of the laser-marked DMC on aluminum and copper foil with direct exposure, diffuse exposure, and polarized exposure in (b) and decoding times of the laser-marked DMCs in (c) and ink-marked DMCs with 12 x 26 DMCs in (d).

The decoding time of the codes is significantly influenced by the code size. For illustration, **Figure 8** shows the decoding time of laser marked DMCs with different cell sizes. The cell size describes the size of an individual module or pixel of the DMC. There were notable variations, particularly for codes with 0.2 mm and 0.5 mm cell size as for the first, resolution becomes critical and for 0.5 mm cell size the thermal distortion by the laser marking process resulted in pronounced waviness and hence reflections and distortions. For this reason, cell sizes between 0.3 mm and 0.4 mm have the shortest decoding times. The experiments regarding readability were repeated with three different code readers. The code reader Cognex DM300, due to its lower resolution and direct exposure, red the same codes more slowly than the other more powerful code readers. This again illustrated that the performance differs significantly between code readers, as the costs do. Nevertheless, it should be noted that all code readers were able to read the codes in less than 100 ms.

DOI: 10.14459/2024mp1764299

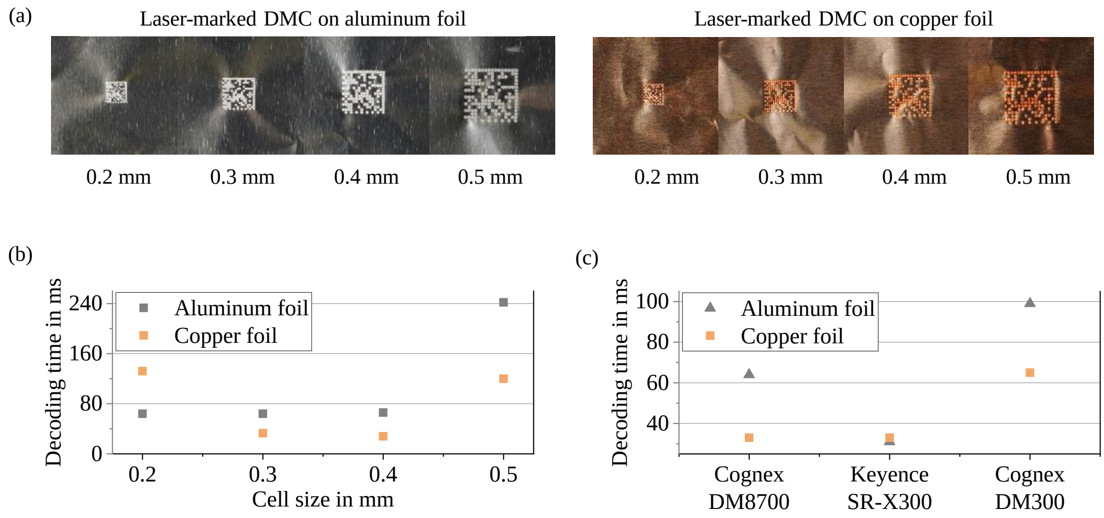

Figure 8: Images of laser-marked DMCs with 16 x 16 modules on aluminum and copper foil with different cell sizes in (a), respective decoding times in (b) and different code readers, maintaining a constant cell size of 0.3 mm in (c).

2.4.2. Selection of suitable code reader

Based on the described parameters and experiments, the following recommendations can be derived:

- Exposure during readout is critical; extraneous light should be avoided while using diffuse or polarized light.
- With reflective current collectors, the illumination on the system may need to be adjusted or the code reader shielded to ensure reliable reading.
- During procurement, attention should be paid to the digital interfaces to enable fast integration into the existing IT infrastructure. It is also advisable to use only one model for all process steps to simplify the integration.
- Additionally, autofocus is beneficial for setup and is often already incorporated.
- The resolution of the camera and the resulting performance of the code readers drives the costs. A high resolution is helpful, but not always necessary.
- Individual tests should be carried out with codes that have already been defined. Only in this way it is guaranteed that the code readers achieve a sufficient decoding frequency.
- Due to the large number of code readers required for a comprehensive T&T system, the code quality should be good to be able to use cost-saving readers.
- A cell size between 0.3 mm and 0.4 mm has proven to be the optimum in terms of decoding time. This applies above all to laser-marked codes, as larger cells also cause greater thermal deformation.
- The readout process is not critical for the web speeds and frequencies that occur in electrode and cell production. It may be necessary to use triggers to guarantee readout within the field of view of the code reader.

3. Example of the implementation of a marker-based traceability system

Exemplarily, the following chapters on ink systems and laser systems showcase the marking technologies employed at the pilot lines of ZSW and *iwb*. Here, only the integration of the marking units is addressed. The description of the construction of the entire traceability systems is detailed in further literature.

3.1. Ink-based marking system

In the context of the research project *TrackBatt*, two continuous inkjet printers (MK-G1000 Continuous Inkjet Printer, Keyence, Osaka, Japan) with two different inks (MK10 and MK20, Keyence, Osaka, Japan) were installed for the

DOI: 10.14459/2024mp1764299

marking of electrodes in the research production line at ZSW. **Figure 9** demonstrates the integration of continuous ink printers into the coating machine at ZSW.

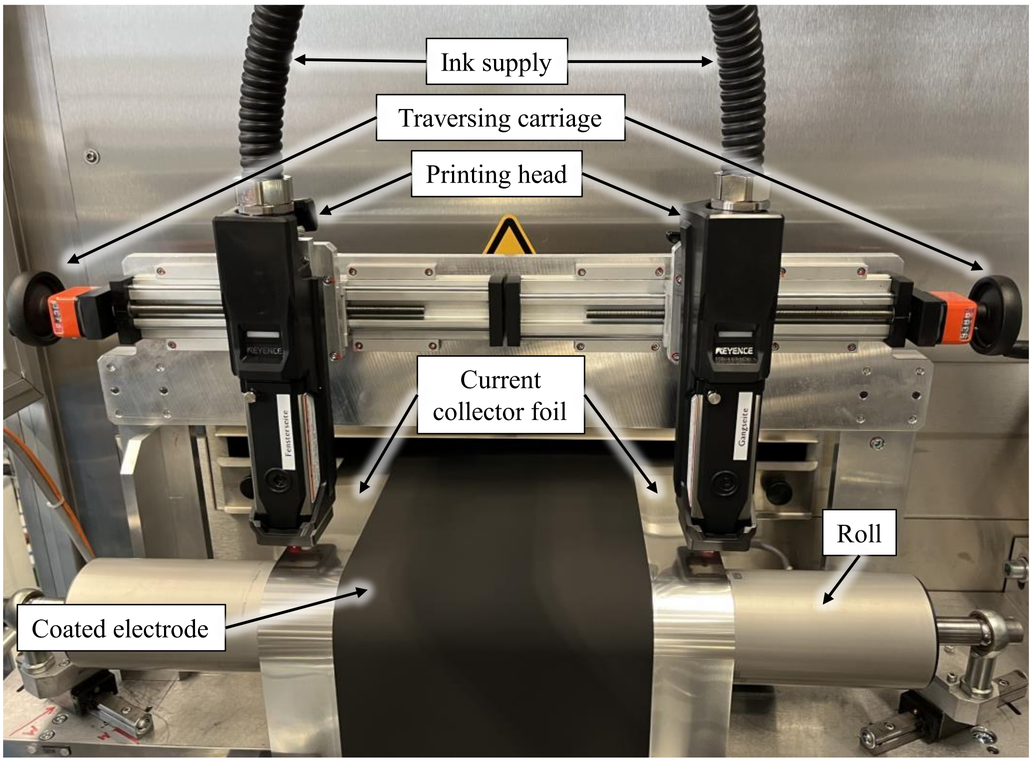

Figure 9: Integration of two continuous ink marking systems into the coating machine at ZSW. The produced electrodes were marked on the current collector foils during the coating process.

Due to typical lengthwise slitting of the electrode after the coating and calendering process, two printers were necessary to mark each electrode side. To mark various foil widths, the marking units were mounted on a traversing carriage, with ink supplied through a pipe. The inkjet marking system exhibited low sensitivity to changes in the marking distance between the ink outlet and the marking object, which could be caused by vibrations in the foil during operation. However, altering the marking distance affected the overall size of the DMC modules, potentially causing issues with reading accuracy later. To address this, the marking units were positioned close to a roll in the system to maintain a constant marking distance during the process. The printers were controlled via the Human-Machine Interface of the coating system, where the code content and marking distances between the codes are specified. Based on the current web speed, the system triggered the printers to maintain the correct distance between the codes. The maximum marking speed is determined by the quantity of DMC modules. At ZSW, a DMC with 12 x 26 modules was employed, enabling a maximum marking speed of 168 m min^{-1} with the utilized system. The operational costs for running the printers include consumables such as ink and solvents, electricity, as well as wearing parts like pumps, filters, and nozzles. During the process, code readers (SR–2000W, Keyence, Japan) were integrated into the coating machine. Coating and drying data for individual electrode sections were adjusted using the meter counter of the machine, ensuring accurate tracing despite web stops and speed changes. Initial steps involved determining distances between sensor points and code readers, which remained fixed values in subsequent tracing calculations. Using this information, sensor data could be clearly assigned to electrode codes in the database. A detailed execution of the traceability system is described in the literature. [16,18]

3.2. Laser-based marking system

As part of the research project *TrackBatt*, a laser marking system (Y.0300-xs, ALLTEC GmbH, Germany) for inline labeling of current collector foils was integrated into the coating machine of the pilot line at *iwb*. In **Figure 10** the integration of the laser system, including the necessary laser housing is shown.

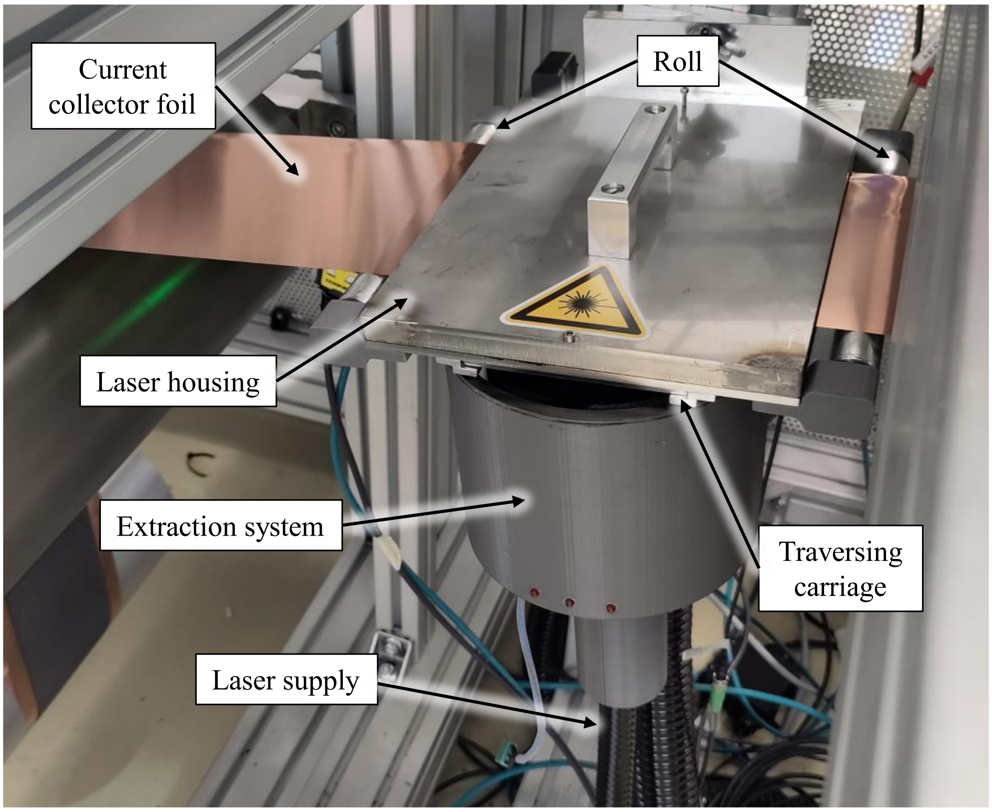

Figure 10: Integration of the laser marking system including the laser housing at *iwb*. The housing ensures that no hazardous laser radiation can escape. Additionally, it incorporates an extraction system to remove any generated particles or vapors. The electrodes were marked on the current collector foils after the coating process.

A custom laser housing was installed in the coating machine to meet all operating requirements for the laser marking system. To ensure smooth and steady movement of the foil, two support rolls were incorporated to hold the foil securely and prevent vibrations. These rolls were linked mechanically to the laser housing to maintain a consistent marking distance and focus. A traversing carriage was integrated to allow manual adjustment of the laser position on the moving foil. Safety measures included a U-shaped enclosure extending over the foil's width to protect operators from laser radiation and an exhaust system to prevent particle contamination on the electrodes. With the help of the laser housing, a marking distance of 81 mm was chosen for the anode and 78 mm for the cathode electrode format. Coating and marking were done at speeds of up to 2 m min^{-1}. Tracking was performed during production, involving reading DMCs and recording timestamps using code readers operated with a continuous trigger at 5 Hz. These timestamps, along with the content of the markings, were stored in a database. Timestamps for specific production steps and sensors were then calculated using a combination of timestamps and meter counters to determine the location and time of electrode sections during coating and drying. Distances between code readers, sensors, and production steps were measured to correct the allocation of sensors and process data based on meter counters[16]. This

DOI: 10.14459/2024mp1764299

allowed for the extraction of time from the meter counter, considering relevant offset values, accommodating potential standstills and changes in web speed. Timestamps were used to allocate process and product parameters to corresponding electrode sections, with sensor and machine parameters stored in distinct databases synchronized to production seconds. The tracing process involved cross-referencing tracking timestamps with process data from sensors and machines, linking information directly or indirectly to electrode sheets, either immediately or after additional processing. While reading DMCs and recording timestamps occurred during production, T&T were performed offline after production to adjust setting parameters. The further detailed execution of the traceability system is described in the literature [16,18]

4. Marker-free system

One approach that is attracting increasing attention in T&T systems is marker-free tracking. In contrast to conventional methods that rely on ID carriers such as DMCs, this method uses alternative technologies to track electrode structure parameters along the process chain without applying physical markings to them to avoid or prevent negative influences of the marking.[11,17] In this context, a marker-free traceability concept requires the extraction of a repeating data pattern and is subject to some limitations and challenges, especially in electrode production.[40] A key challenge is recognizing the intermediate products based on the changed surfaces after the calendaring process, as well as during the cutting of the electrode and the associated reduction in the measured values available for tracking.

For instance, WESSEL et al. carried out marker-free tracking based on coating defects. This involved taking images of the electrode before and after calendering and extracting feature values from the images. By comparing the images and the occurrence of specific defect patterns, in this case pinholes, it was possible to find all defective sections with a high degree of accuracy. The disadvantage is that surface defects or similar visible structures are needed for tracking, but these can be altered or even disappear due to calendering.[41] RIEXINGER et al. pursued a different approach. Here, the challenge of the changing electrode structure was avoided by utilizing the surface properties of the current collector foil. A camera-based system was developed to identify the individual surface structure of the foils. For this purpose, the recorded images are converted into numerical identification codes and stored in a database. These can be found again by re-measuring, even if the electrode has already been separated. It is also pointed out that the technology has only been implemented in an industrial production line to track discrete objects. [41]

A third approach to marker-free tracking is based on the use of quality features measured inline. This approach uses certain quality features such as gloss, colour, or, for example, mass loading to identify specific electrode sections.[42] To investigate this approach in the scope of this work, the ultrasonic extension meter from Mesys GmbH was used, which measures one of the most important quality parameters of the electrode coating and is not influenced by subsequent processes. Due to the nine array sensors fixed positions and high data resolution, this system is ideal for investigating the requirements for sensor systems for extracting a fingerprint approach.

A 7.5 m long and 0.2 m wide single-sided cathode with an average surface weight of 30 mg cm^{-2} was measured twice to generate two data sets. The electrode was produced with the first 4 meters manufactured consistently, while defects were intentionally introduced in the last 3 meters by varying the doctor blade gap. The resulting scattering of the process and the influence on the repeatability is given in **Figure 11**. Based on this, the sections were divided into four blocks to be able to analyse the impact on the matching accuracy in more detail. In **Figure 11a** both measurements on top of each other and the standard deviation to visualize the process scatter of the individual data blocks are shown. In **Figure**

DOI: 10.14459/2024mp1764299

11b the difference between the two measurements to visualize the measurement's repeatability in the individual blocks is presented. The standard deviation shown indicates the deviation of the measurements from each other.

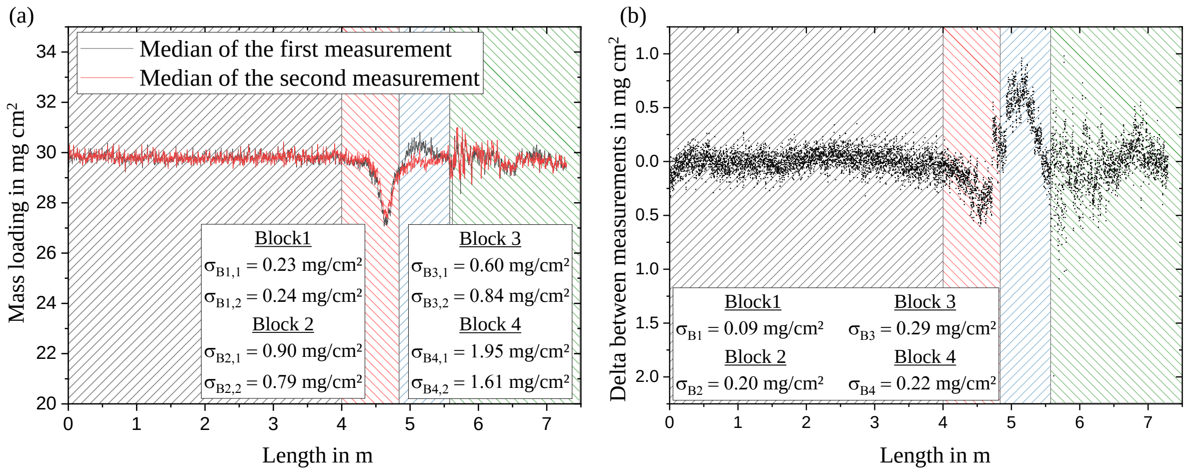

Figure 11: Data presentation of the raw data for visualization of scattering in the individual sections. Illustration of measurements 1 and 2 with a standard deviation of the individual measurements in the respective blocks in (a). Illustration of the difference between the measurement values to visualize the repeatability of the measurement in (b).

For matching the electrode sections, the first measurement was used as the baseline for the assignment in data set 1. Data set 2 was divided into objects of different lengths (data blocks), representing the sections to be matched and searched for in data set 1. By processing the data sets in advance, the required areas were identified. This enabled subsequent checking of the matching process and determination of hit rates and false positive rates. The correlation similarities were used to calculate the similarity between data set 1 and the respective search object. Here, data set 1 is iteratively compared with the data of the respective search object, and the area of highest similarity is located. The covariance cov between the individual columns of both data blocks was calculated. First, the mean values $\bar{X}$ and $\bar{Y}$ from the columns investigated are determined and are then calculated with the individual rows X_i and Y_i within the columns, shown in **Equation 1**.

$$cov = \frac{1}{n}\sum_{i=1}^{n}(X_i - \bar{X})(Y_i - \bar{Y}) \qquad (1)$$

The covariance measures how two variables change together. It is positive if both variables tend to increase or decrease simultaneously. If one variable increase while the other decreases, the covariance is negative. The correlation coefficient r is then calculated as the covariance between data blocks 1 and 2 divided by the product of the standard deviations of data blocks 1 and 2, shown in **Equation 2**. The correlation coefficient is then averaged across all columns.

$$r = \frac{cov(X,Y)}{\sqrt{(\sum_{i=1}^{n}(X_i - \bar{X})^2)(\sum_{i=1}^{n}(Y_i - \bar{Y})^2)}} \qquad (2)$$

This value ranged from –1 to 1. A score of 1 indicates a perfect positive linear relationship, –1 indicates a perfect negative linear relationship, and 0 indicates no linear relationship.

DOI: 10.14459/2024mp1764299

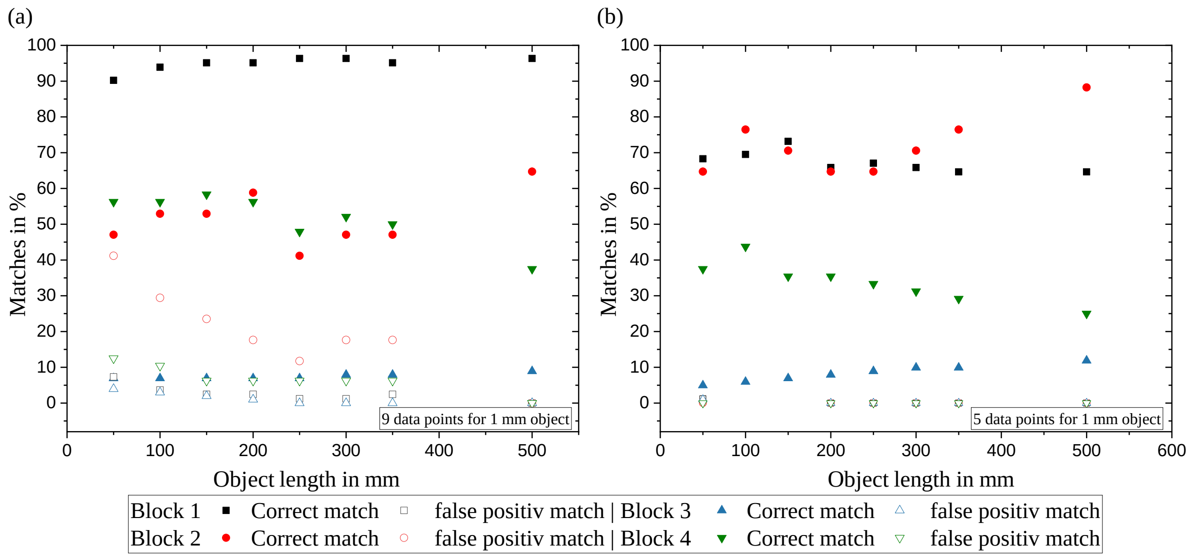

Figure 12: Illustration of the matching results with false positive rates: (a) results calculated based on all data in (a); results based on a reduced data set in (b).

Figure 12 shows that different matching accuracies and false positive rates were calculated for the different areas of the data set. The main reason for this is the scattering of the measurement data by the process, but above all, the repeatability of the measurement, i.e., the similarity of the data to each other. Furthermore, as shown in **Figure 12b**, the data reduction reduces the matching accuracy. Based on the calculations, the following key influencing parameters can be defined:

Object length: The longer the object and, therefore, the number of available data points, the lower the false positive rates. The matching rates are only slightly influenced.

Number of measured values: If the number of measured values is reduced, the matching result deteriorates drastically from 96 % to 60 % with a simultaneously high false positive rate, see **Figure 12a and b** Block 1. The reason for this is the flattening of the data and thus the reduction of the characteristic features of the data set.

The similarity of the data set: As can be seen from **Figure 11b**, there is a direct correlation between the standard deviation shown of the measurement difference and the matching results. From a measurement deviation between the data sets larger than 0.1 mg cm^{-2}, a direct decrease in the matching accuracy occurs, and at a value larger than 0.22 mg cm^{-2}, only very few sections can be found.

Process variation: **Figure 12** shows that a decrease in the matching accuracy and a false positive rate occurs for all data blocks except block one due to the increase in the standard deviation of production. The main reason for this is not the direct influence of the process variation on the matching but the impact of the process variation on the repeatability of the sensor.

Consequently, accepting a low level of misallocation, it is possible to implement a marker-free T&T system. However, a marker-free T&T system needs the sensors for detection of the fingerprints in every process step. As a result, the system costs quickly exceed the costs of a marker-based system. This mainly depends on the sensors used and the process effort for the assignment.

5. Conclusion

For a comprehensive T&T system in battery cell production, it is crucial to uniquely identify intermediate products. This enables a clear assignment of the production data and a characterization of the intermediate products based on these. The aim of this work was to present different identification options for intermediate products in battery cell production. Based on the results of the research project *TrackBatt* (Grant Reference: 03XP0310), ink-based, laser-based, and non-marking methods were investigated and discussed regarding their suitability in battery cell production. The fundamental distinction between marking-based and non-marking methods lies in integrating a physical code into the process chain, which is read at crucial points in the process. In non-marking methods, so-called fingerprints on the intermediate products are recognized, which can be unmistakably identified. For ink-based and laser-based methods, it is noteworthy that both variants require constructive efforts for inline use. This eliminates an additional marking process step, and the marking can be adapted to the corresponding cell format to be produced. It has been found that ink-based methods are significantly easier and faster to integrate compared to a laser-based system. The marking itself does not interact with the current collector foils and exhibits high contrast, ensuring good readability. However, care should be taken to prevent the ink-based marking from encountering electrolytes, as it dissolves in the electrolyte solvents and can contaminate them. A negative impact on cell performance cannot be entirely ruled out. To avoid contact between the ink-based marking and the electrolyte, it is recommended to place the marking on areas of the current collector flags that are subsequently removed in the assembly steps. Data assignment is done through the cell housings and remains consistent throughout the process chain. Laser-based methods offer much more flexibility in applying individual markings but require protection against hazardous laser radiation. This can be achieved through laser safety housing or appropriate enclosures. Furthermore, attention should be paid to the effort required for laser application on the used foil to create legible codes. Also, the investment costs are higher compared to ink-based methods. However, both marking-based methods have proven suitable for use in battery cell production. Non-marking methods do not require the physical introduction of a DMC into the process chain and, therefore, do not require investigations into unintended interactions between processes and markings. While it is generally possible to recognize intermediate products using integrated sensors, recognition at each process step requires sophisticated sensor technology to identify the fingerprints again. Therefore, a non-marking method is only suitable if the corresponding sensor technology can be scaled across all process steps.

6. Summary and Outlook

To establish a comprehensive T&T system in battery cell production, it's crucial to implement a distinct marking system for intermediate products, a step that should already be integrated into the electrode manufacturing process. This paper presents a guideline aimed at integrating either laser-based, ink-based, or marking-less methods to achieve this goal. The integration process is structured into four steps. In Step 1, the initial task involves defining the boundary conditions of the T&T system. This entails recognizing that the T&T system must seamlessly integrate into the electrode manufacturing phase of battery production. Determining these boundary conditions hinges on various factors such as the material properties of current collector foils, process specifications, the required data to be stored, and the configurations of the electrodes. Moving to Step 2, attention turns to code design. Here, various coding options, such as DMC or QR codes, are evaluated. Before selecting an appropriate code, it's essential to establish the specific requirements for code design. Step 3 focuses on the practical application of markings or DMCs through either ink-based or laser-based systems. These methods are already extensively utilized in the industry for labeling components in T&T applications. Given the diverse requirements and respective advantages and disadvantages of these systems, this paper offers a sophisticated analysis. However, both methods share the fundamental characteristic of storing unique information within the code itself, facilitating the differentiation of intermediate products. Finally, Step 4 addresses the decoding process of the applied markings. Code readers available in the industry vary not only in their functionalities but also significantly in their costs. Thus, it's prudent to carefully assess the requirements for the code reader to ensure the procurement of suitable devices without incurring unnecessary expenses. Finally, the integration of the marking technologies into the two research production lines of the *iwb* and the ZSW were presented as an example. The T&T systems are already being used for cell production in their production lines.

Acknowledgements

The presented results were gathered within the research project "TrackBatt" (03XP0310), funded by the German Federal Ministry of Education and Research (BMBF). We would like to thank the BMBF and the Project Management Organization Jülich for the trustful cooperation and the financial support.

References

[1] H.-O. Pörtner, D.C. Roberts, M. Tignor, E.S. Poloczanska, K. Mintenbeck, A. Alegría, M. Craig, S. Langsdorf, S. Löschke, V. Möller, A. Okem, B. Rama (eds.) (Intergovernmental Panel on Climate Change), *Climate Change 2022 – Impacts, Adaptation and Vulnerability*, Cambridge University Press, **2023**.

[2] L. S. Martins, L. F. Guimarães, A. B. Botelho Junior, J. A. S. Tenório, D. C. R. Espinosa, *Journal of environmental management* **2021**, *295*, 113091.

[3] A. Kwade, W. Haselrieder, R. Leithoff, A. Modlinger, F. Dietrich, K. Droeder, *Nat Energy* **2018**, *3*, 290–300.

[4] F. Duffner, L. Mauler, M. Wentker, J. Leker, M. Winter, *International Journal of Production Economics* **2021**, *232*, 107982.

[5] J. Schnell, G. Reinhart, *Procedia CIRP* **2016**, *57*, 568–573.

[6] N. Wittine, S. Wenzel, C. Kern, R. Refflinghaus, T. Trostmann, *Introduction of Traceability into the Continuous Improvement Process of SMEs*, Hannover : publish-Ing, **2020**.

[7] J. Schnell, C. Nentwich, F. Endres, A. Kollenda, F. Distel, T. Knoche, G. Reinhart, *Journal of Power Sources* **2019**, *413*, 360–366.

[8] M. Thomitzek, O. Schmidt, T. Abraham, F. Cerdas, F. Röder, U. Krewer, C. Herrmann, *Procedia CIRP* **2021**, *104*, 1059–1064.

[9] A. Turetskyy, S. Thiede, M. Thomitzek, N. von Drachenfels, T. Pape, C. Herrmann, *Energy Tech* **2020**, *8*.

[10] S. Thiede, A. Turetskyy, A. Kwade, S. Kara, C. Herrmann, *CIRP Annals* **2019**, *68*, 463–466.

[11] G. Riexinger, J. P. Doppler, C. Haar, M. Trierweiler, A. Buss, K. Schöbel, D. Ensling, T. Bauernhansl, *Procedia CIRP* **2020**, *93*, 125–130.

[12] J. Wessel, A. Turetskyy, O. Wojahn, C. Herrmann, S. Thiede, *Procedia CIRP* **2020**, *93*, 162–167.

[13] O. Meyer, C. Weihs, S. Mähr, H.-Y. Tran, M. Kirchhof, S. Schnackenberg, J. Neuhaus-Stern, S. Rößler, W. Braunwarth, *Energy Tech* **2020**, *8*.

[14] J. Wessel, A. Schoo, A. Kwade, C. Herrmann.

[15] A. Sommer, M. Leeb, S. Haghi, F. J. Günter, G. Reinhart, *Procedia CIRP* **2021**, *104*, 1011–1016.

[16] A. Sommer, S. Bazlen, H.-Y. Tran, M. Leeb, J. Wachter, W. Braunwarth, R. Daub, *Energy Tech* **2024**.

[17] A. Sommer, M. Leeb, L. Weishaeupl, R. Daub, *Batteries* **2023**.

[18] A. Sommer, S. Bazlen, H.-Y. Tran, W. Braunwarth, R. Daub, *Procedia CIRP* **2023**, *120*, 171–176.

[19] A. Sommer, J. Wachter, S. Grabmann, R. Daub, *Batteries & Supercaps* **2024**. (accepted article)

[20] M. Ank, A. Sommer, K. Abo Gamra, J. Schöberl, M. Leeb, J. Schachtl, N. Streidel, S. Stock, M. Schreiber, P. Bilfinger et al., *J. Electrochem. Soc.* **2023**, *170*, 120536.

[21] S. Stock, J. Hagemeister, S. Grabmann, J. Kriegler, J. Keilhofer, M. Ank, J. L. Dickmanns, M. Schreiber, F. Konwitschny, N. Wassiliadis et al., *Electrochimica Acta* **2023**, *471*, 143341.

[22] ISO/IEC 16022:2006, *Information technology — Automatic identification and data capture techniques — Data Matrix bar code symbology specification*.

[23] C. Moss, S. Chakrabarti, D. W. Scott in *2013 IEEE Aerospace Conference*, IEEE, **2013**, 1–12.

[24] L. Lazov, A. Atanasov, N. Angelov, *CM* **2011**, *2*, 13–17.

[25] L. Lazov, H. Deneva, P. Narica, *ETR* **2015**, *1*, 108.

[26] M. W. Sigrist, *Laser: Theorie, Typen und Anwendungen*, Springer Berlin Heidelberg, Berlin, Heidelberg, **2018**.

[27] G. D. Martin, S. D. Hoath, I. M. Hutchings, *J. Phys.: Conf. Ser.* **2008**, *105*, 12001.

[28] S. Magdassi (Ed.) *The chemistry of inkjet inks*, World Scientific, Singapore, **2010**.

[29] L.-C. Chen, D. Liu, T.-J. Liu, C. Tiu, C.-R. Yang, W.-B. Chu, C.-C. Wan, *Journal of Energy Storage* **2016**, *5*, 156–162.

[30] M. Schmitt, P. Scharfer, W. Schabel, *J Coat Technol Res* **2014**, *11*, 57–63.

[31] J. Eichler, H.-J. Eichler, *Laser. Bauformen, Strahlführung, Anwendungen; mit 57 Tabellen, 164 Aufgaben und vollständigen Lösungswegen*, Springer, Berlin, Heidelberg, **2006**.

[32] P. Fan, M. Zhong, L. Li, P. Schmitz, C. Lin, J. Long, H. Zhang, *Journal of Applied Physics* **2013**, *114*, 83518.

[33] M. Gedvilas, *JLMN* **2014**, *9*, 267–270.

[34] G. Raciukaitis, M. Brikas, P. Gecys, M. Gedvilas in *SPIE Proceedings* (Ed.: C. R. Phipps), SPIE, **2008**, 70052L.
[35] Y.-Y. Kim, J.-Y. Joo, J.-M. Kim, S.-K. Lee, *Sensors (Basel, Switzerland)* **2021**, *21*.
[36] W. M. Steen, *Laser material processing*, Springer, London, Berlin, Heidelberg, **2003**.
[37] I. Balchev, N. Minkovski, T. Marinova, M. Shipochka, N. Sabotinov, *Materials Science and Engineering: B* **2006**, *135*, 108–112.
[38] J. Winter, M. Spellauge, J. Hermann, C. Eulenkamp, H. P. Huber, M. Schmidt, *Optics express* **2021**, *29*, 14561–14581.
[39] C. Connolly, *Assembly Automation* **2005**, *25*, 182–187.
[40] G. Riexinger, D. J. Regina, C. Haar, T. Schmid-Schirling, I. Landwehr, M. Seib, J. Lips, S. Fehrenbach, J. Stübing, D. Carl et al. in *ARENA2036* (Eds.: N. Kiefl, F. Wulle, C. Ackermann, D. Holder), Springer International Publishing, Cham, **2023**, pp. 344–353.
[41] A. Schoo, R. Moschner, J. Hülsmann, A. Kwade, *Batteries* **2023**, *9*, 111.
[42] J. Wessel, A. Schoo, A. Kwade, C. Herrmann, *Energy Tech* **2023**, *11*.